# Characteristics of $Sb_6Te_4/VO_2$ Multilayer Thin Films for Good Stability and Ultrafast Speed Applied in Phase Change Memory *

Yi-Feng Hu(胡益丰)[1,3,4**], Xuan Guo(郭璇)[1], Qing-Qian Qiu(仇庆前)[2], Tian-Shu Lai(赖天树)[2]

[1]*School of Mathematics and Physics, Jiangsu University of Technology, Changzhou 213000*

[2]*State Key Laboratory of Optoelectronic Materials and Technology, School of Physics, Sun Yat-Sen University, Guangzhou 510275*

[3]*State Key Laboratory of Silicon Materials, Zhejiang University, Hangzhou 310027*

[4]*Key Laboratory of Microelectronic Devices & Integrated Technology, Institute of Microelectronics, Chinese Academy of Sciences, Beijing 100029*

(Received 27 April 2018)

*The $Sb_6Te_4/VO_2$ multilayer thin films are prepared by magnetron sputtering and the potential application in phase change memory is investigated in detail. Compared with $Sb_6Te_4$, $Sb_6Te_4/VO_2$ multilayer composite thin films have higher phase change temperature and crystallization resistance, indicating better thermal stability and less power consumption. Also, $Sb_6Te_4/VO_2$ has a broader energy band of 1.58 eV and better data retention (125°C for 10 y). The crystallization is suppressed by the multilayer interfaces in $Sb_6Te_4/VO_2$ thin film with a smaller rms surface roughness for $Sb_6Te_4/VO_2$ than monolayer $Sb_4Te_6$. The picosecond laser technology is applied to study the phase change speed. A short crystallization time of 5.21 ns is realized for the $Sb_6Te_4$(2 nm)/$VO_2$ (8 nm) thin film. The $Sb_6Te_4/VO_2$ multilayer thin film is a potential and competitive phase change material for its good thermal stability and fast phase change speed.*

*PACS:* 68.05.Cf, 68.55.−a, 68.65.−k DOI: 10.1088/0256-307X/35/9/096801

With the increase of consumer electronics, the demand for volatile memory has increased dramatically.[1,2] Flash is now the mainstream of the non-volatile memory market, but flash has several drawbacks such as long operation time, high switching voltage and charge storage limitation. These facts make it unable to meet the law of proportional reduction when the size is very small.[3−5] Phase change memory (PCM) is regarded as the most promising alternative memory due to its fast reading and writing speed, high density storage capacity and compatible with Complementary metal oxide semiconductor (CMOS).[6−9] To solve the problems of large operation current and thermal interference, the whole development trend of PCM is in the three-dimensional nanometer scale direction. The sulfur compound semiconductor is a key portion of the phase change memory currently, and it directly determines the performance of the PCM device.[10,11]

At present, Sb-rich $Sb_6Te_4$ is widely used in PCM research, but $Sb_6Te_4$ has some limitation such as low crystallization temperature (∼120°C) and poor data retention (∼57°C for 10-y), which cannot meet the requirements of high density storage in the future big data age.[12−14] Therefore, the doping is used to improve the thermal stability, such as Si,[15] $S_C$,[16] W,[17] and Cu.[18] However, it is found that Si doping into $Sb_6Te_4$ can cause the change in crystallization mechanism of doped $Sb_6Te_4$ films from growth dominant to nucleation dominant, which reduces the crystallization rate although Si doping could enhance the thermal stability and resistance.

Recently, the nanocomposite multilayer phase change films are attracting more and more attention because they can provide more control parameters (film thickness, periodicity, cycle number of periodicity) except for composition. Some investigators find that multilayer phase change materials, such as $Ge_{10}Sb_{90}/SiO_2$,[19] $SnSb_4/Ga_3Sb_7$,[20] $SnSb_4/Ge$,[21] can increase the reversible phase-change speed and decrease the whole operation power consumption because they can combine the preponderance as well as complement shortcomings of each materials.

In this Letter, we investigate the characteristics of the $Sb_6Te_4/VO_2$ (ST/VO) multilayer thin films prepared by means of the magnetron sputtering method. Thereinto, Sb-rich $Sb_6Te_4$ (ST) phase-change films have a fast switching speed and low crystallization temperature. Oxide material $VO_2$ (VO) has no phase-change characteristic, while it can enhance the resistance as well as thermal stability of the composite multilayer films. Thus when $Sb_6Te_4$ and $VO_2$ are integrated by multilayer composite, a better comprehensive performance can be expected.

Before sputtering the films, $Si/SiO_2$ substrates were washed with distilled water after ultrasonic cleaning in ethanol. Then, $Si/SiO_2$ substrates were glued onto sample plates with double faced adhesive

*Supported by the National Natural Science Foundation of China under Grant No 11774438, the Natural Science Foundation of Jiangsu Province under Grant No BK20151172, the Qing Lan Project, the Opening Project of State Key Laboratory of Silicon Materials under Grant No SKL2017-04, the Opening Project of Key Laboratory of Microelectronic Devices and Integrated Technology of Chinese Academy of Sciences, and the Postgraduate Research and Practice Innovation Program of Jiangsu Province under Grant No SJCX18_1024.

**Corresponding author. Email: hyf@jsut.edu.cn

© 2018 Chinese Physical Society and IOP Publishing Ltd

tape. Subsequently, the sample plates were placed in the vacuum chamber of the radio-frequency (rf) magnetron sputtering instrument. The $Sb_6Te_4$ and $VO_2$ targets were placed in the corresponding target. The purity of $Sb_6Te_4$ and $VO_2$ targets was 99.999%. To compare with ST/VO multilayer thin films, pure $Sb_6Te_4$ monolayer thin film was prepared at the same time. The thickness of thin films was controlled by the sputtering time. The pressure of the magnetron sputtering chamber in the film sputtering was 0.4 Pa, with a flow of 30 sccm and an rf power of 30 W.

The thickness of the thin films was measured using a form talysruf profiler (ET-4000M). The resistance as a function of temperature was measured using the *in situ* measurement with a heating rate of 30℃/min. The temperature was controlled by a TP 94 temperature controller (Linkam Scientific Instruments Ltd, Surrey, UK). The band gap was obtained by measuring the reflectivity of thin film by means of a near-infrared spectrophotometer. The activation energy and data retention temperature for 10 y can be further gained by measuring the isothermal crystallization curve. Structure properties of as-deposited and annealed ST/VO multilayer thin films were studied using x-ray diffraction (XRD). Phase-change times in the crystallization and amorphization process were examined by the picosecond laser technology. The images of the film surface were measured by an atomic force microscope (AFM).

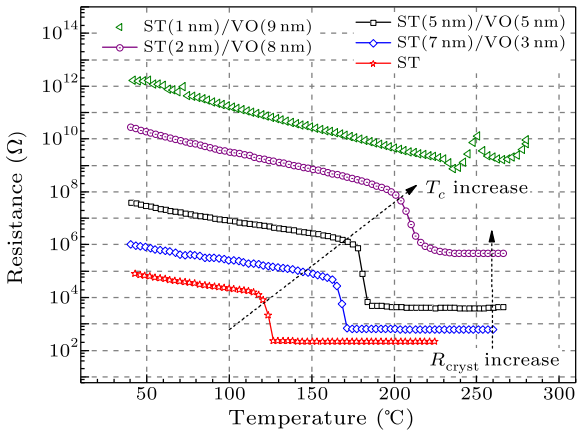


**Fig. 1.** The resistance as a function of temperature for ST/VO composite multilayer thin films.

To exclude the influence of the total thickness and the periodicity of the multilayer film, all the ST/VO multilayer thin films were set with 50 nm thickness and 5 periods. The resistance of the ST monolayer and ST/VO multilayer thin films with different thickness ratios as a function of temperature ($R$–$T$) is shown in Fig. 1. Firstly, the resistance of all the films decreases slowly with the increase of temperature. A sharp resistance drop happens at the crystallization temperature $T_c$. With the increase of the relative thickness of the VO layer in the ST/VO multilayer thin films, $T_c$ increases from 164℃ of ST(7 nm)/VO(3 nm) to 179℃ of ST(5 nm)/VO(5 nm), 204℃ of ST(2 nm)/VO(8 nm), which are all higher than that of ST (120℃). Obviously, the thermal stability has been enhanced by adding the thickness of VO layers. Meanwhile, there is at least one order of magnitude difference between amorphous and crystalline state resistance of the above three ST/VO multilayer thin films, which can guarantee there is enough distinguishability in the PCM device. Moreover, the crystallization resistance increases from 182 Ω of ST to $4 \times 10^5$ Ω of ST(2 nm)/VO(8 nm). According to the formula $Q = I^2 \cdot R \cdot t$, a higher resistance is conducive to improving the self-heating efficiency, resulting in a decrease of power consumption as well as a faster phase change speed. Significantly, except the slow resistance decrease due to semiconductor-like behavior at first, no obvious resistance mutation is observed for ST(1 nm)/VO(9 nm), which implies that the phase transition is inhibited due to the excess VO material.

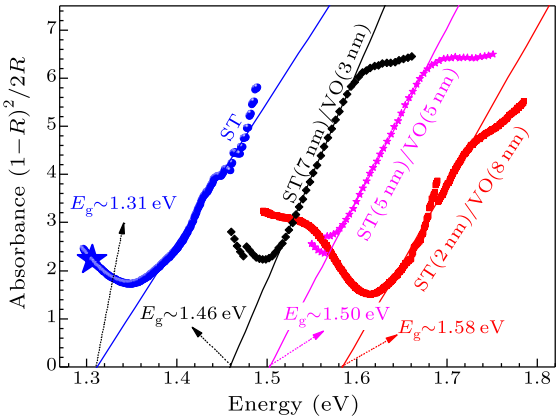


**Fig. 2.** The Kubelka–Munk function of the amorphous ST monolayer and the ST/VO multilayer thin films.

In Fig. 2, the UV-visible-NIR spectrophotometry with the wavelength range from 200 to 2500 nm is used to measure the diffuse reflectivity spectra of the amorphous ST monolayer and the ST/VO multilayer thin films. By extrapolating the absorption edge onto the energy axis, the band gap energy ($E_g$) can be obtained. Based on the Kubelka–Munk function (K-M), the conversion of the reflectivity to absorbance data was realized,[22]

$$K/S = (1-R)^2/(2R), \tag{1}$$

where $R$ is the reflectivity, $K$ is the absorption coefficient, and $S$ is the scattering coefficient. Figure 2 shows that $E_g$ for the ST monolayer and the ST (7 nm)/VO (3 nm), ST (5 nm)/VO (5 nm), ST (2 nm)/VO (8 nm) multilayer thin films are 1.31, 1.46, 1.50, and 1.58 eV, respectively. Generally, a large optical band gap indicates decreasing electrical conductivity because the electrons' transition from the valence band to the conduction band is difficult. Thus, the activation energy for electrical conductivity increases. This finding is supported by the change trends of resistance curves in Fig. 1.

To further evaluate the reliability, the isothermal crystallization was carried out for the phase change

films. Generally, the Arrhenius model can briefly characterize the relationship between the failure-time and test temperature. The plots of logarithm failure time versus $1/k_bT$, exhibited in Fig. 3, fit a linear Arrhenius relationship because of its thermal activation nature. The linear relationship is expressed as[23]

$$t = \tau_0 \exp(E_a/k_bT), \tag{2}$$

where $t$, $\tau_0$, $E_a$, $k_b$, and $T$ are failure time, a pre-exponential factor depending on the film's properties, activation energy of crystallization, Boltzmann constant, and absolute temperature, respectively. As we can see in Fig. 3, the extrapolated temperatures of 10-year data retention lifetime for the ST, ST (7 nm)/VO (3 nm), ST (5 nm)/VO (5 nm), ST (2 nm)/VO (8 nm) multilayer thin films are 57, 75, 112, and 125℃, respectively. Accordingly, the activation energy of crystallization ($E_a$) increases monotonically from 1.37 eV of ST to 4.67 eV of ST (2 nm)/VO (8 nm). From the above data, it shows that the data retention of phase change film is greatly improved by adding VO composite layers.

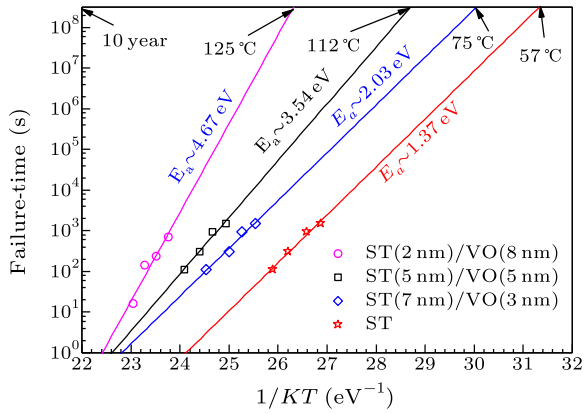


**Fig. 3.** Plots of failure times as a function of reciprocal temperature for the ST/VO composite multilayer thin films.

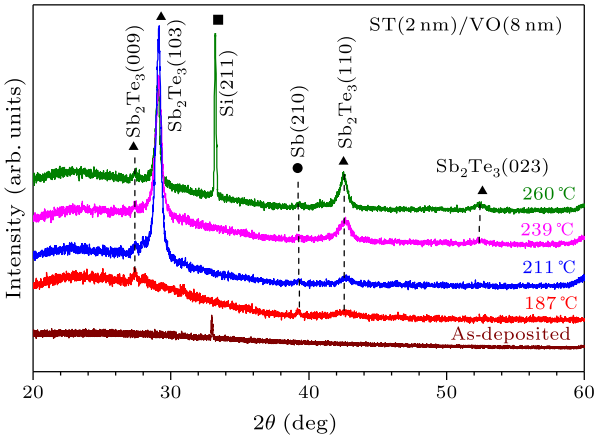


**Fig. 4.** XRD patterns of ST (2 nm)/VO (8 nm) thin films annealed at different temperatures for 30 min in Ar atmosphere.

Figure 4 represents the x-ray diffraction (XRD) images of ST (2 nm)/VO (8 nm) multilayer thin film annealed at different temperatures. As is shown in Fig. 4, the as-deposited ST (2 nm)/VO (8 nm) thin film has no diffraction peaks, indicating an amorphous structure. When the annealing temperature reaches up to 187℃, two weak diffraction peaks of (009) and (110) belonging to the $Sb_2Te_3$ phase appear. A strong diffraction peak (103) of the $Sb_2Te_3$ phase is observed in the above 211℃ annealed films. Furthermore, a laigh peak of $Sb_2Te_3$ (023) can be discerned in the 239℃ and 260℃ annealed films. Furthermore, no other alloy phases are observed in the annealed ST (2 nm)/VO (8 nm) film, indicating the stoichiometric ratio $Sb_2Te_3$ is the main phase form. It should be noted that the Sb (210) phase exists in all the annealed ST (2 nm)/VO (8 nm) films, indicating that the Sb element is excessive in the $Sb_6Te_4$ materials. The dispersed Sb-Sb bonds are easily broken in the crystallization process and act as heterogeneous nucleating agents.[24] This provides a large number of starting positions for crystallization and accelerates the phase change of the material.

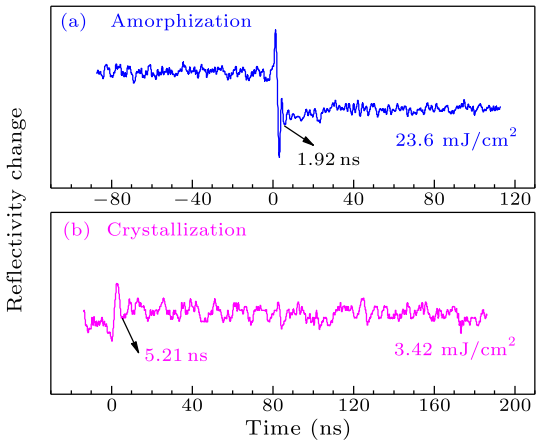


**Fig. 5.** Reflectivity evolutions in the amorphization and crystallization processes for the ST (2 nm)/VO (8 nm) multilayer thin film.

Except for the current pulse stimulation, phase change can be realized by the superlaser. In the irradiation of laser, the reflectivity of phase change materials can have a great change due to internal structure change. Figures 5(a) and 5(b) show the reversible reflectivity evolution of amorphization and crystallization for the ST (2 nm)/VO (8 nm) film at different irradiated energy densities. In Fig. 5(a), the reflectivity decreases to a smaller value with an irradiation intensity of 23.6 mJ/cm$^2$, corresponding to the crystalline-to-amorphous transition. The amorphization time is 1.92 ns. Adversely, when a laser pulse of 3.42 mJ/cm$^2$ is applied, the crystallization happens with the reflectivity jump to a higher value. The crystallization time, generally defined as the criteria to evaluate the phase change speed, is 5.21 ns, which is much shorter than that of $Ge_2Sb_2Te_5$ (39 ns).[25] This result demonstrates that the ST (2 nm)/VO (8 nm) multilayer film has an ultrafast phase change speed,

except good thermal stability.

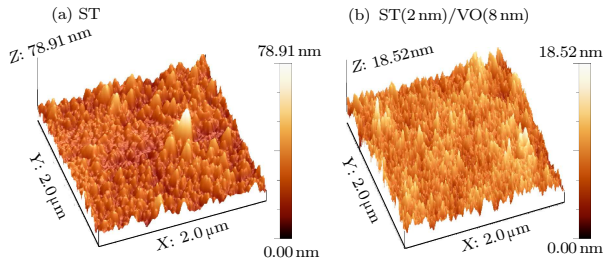


**Fig. 6.** AFM topographic images for (a) ST and (b) ST (2 nm)/VO (8 nm) thin films annealed at 280℃ for 30 min.

In Fig. 6, an atomic force microscope (AFM) is used to measure the surface morphology of the thin films. Figures 6(a) and 6(b) represent the three-dimensional morphological images of the ST and ST (2 nm)/VO (8 nm) thin films after annealing at 280℃ for 30 min. The crystallinity of ST is better than ST (2 nm)/VO (8 nm), which further implies that the crystallization process of ST (2 nm)/VO (8 nm) is suppressed and it will reduce the grain size and produce more grain boundaries. It has been reported that more grain boundaries affect the transmission of the carriers and increase the resistivity, leading to reducing the RESET power consumption. The rms roughness is an important parameter for the phase-change thin film. Here the rms roughnesses for the ST (2 nm)/VO (8 nm) and ST thin films are 2.36 and 10.32 nm, respectively. The smaller change of surfaceness before and after the crystallization of phase-change materials will be beneficial to the contact between the electrode and phase change layer, which will improve the durability properties of the PCM device.

Compared with the ST monolayer thin film, the ST/VO multilayer thin films have more superior characteristics. The crystallization temperature and ten-year data retention temperature for the ST (2 nm)/VO (8 nm) multilayer thin film are 204℃ and 125℃, which are higher than those of the ST monolayer thin film. The energy band is broadened to 1.58 eV after the adding of VO layers. The XRD pattern shows that $Sb_2Te_3$ and Sb phases coexist in the ST (2 nm)/VO (8 nm) multilayer thin film. When a laser irradiation energy of 3.42 mJ/cm$^2$ is applied, the ST (2 nm)/VO (8 nm) multilayer thin film only has a 5.21 ns to realize the amorphous-to-crystalline transition, which is much faster than $Ge_2Sb_2Te_5$. Moreover, the ST (2 nm)/VO (8 nm) thin film has a smoother surface with the rms roughness of 2.36 nm due to the restraint of crystallization. The results show that the ST/VO multilayer thin film has splendid and potential applications in PCM due to its high thermal stability, lower power consumption, and good endurance.

## References

[1] Hu Y F, Zhu X Q, Zou H, Zheng L, Song S N and Song Z T 2017 *J. Alloys Compd.* **696** 150
[2] Yang C, Liu L B, Yin S Y and Wei S J 2014 *Sci. Chin. Ser. G* **57** 2214
[3] Ren K, Li R H, Chen X, Wang Y, Shen J B, Xia M J, Lv S L, Ji Z G and Song Z T 2018 *Appl. Phys. Lett.* **112** 073106
[4] Qian H, Tong H, He M Z, Ji H K, Zhou L J, Xu M and Miao X S 2018 *Sci. Rep.* **8** 486
[5] Hatayama S, Sutou Y, Shindo S, Saito Y, Song Y H, Ando D and Koike J 2018 *ACS Appl. Mater. Interfaces* **10** 2725
[6] Zou H, Zhu X Q, Hu Y F, Sui Y X, Zhang J H and Song Z T 2017 *J. Mater. Sci.: Mater. Electron.* **28** 17719
[7] Zhu W L, Wen T, Hu Y F, Liu X Y, Gu D, Lai T S and Zhai J W 2017 *J. Alloys Compd.* **723** 936
[8] Hu Y F, You H P, Zhu X Q, Zou H, Zhang J H, Song S N and Song Z T 2017 *J. Non-Cryst. Solids* **457** 141
[9] Wu W H, He Z F, Chen S, Zhai J W, Song S N and Song Z T 2017 *J. Phys.* D **50** 095602
[10] Wang G, Zhang Y W, Liu P, Wang J X, Nie Q H and Shen X 2018 *Mater. Lett.* **213** 342
[11] Meng Y, Wu L C, Song Z T, Wen S, Jing M H, Wei J S, Wang Y 2017 *Mater. Lett.* **201** 109
[12] He Z F, Wu W H, Liu X Y, Zhai J W, Lai T S, Song S N and Song Z T 2016 *Mater. Lett.* **185** 399
[13] Zhu C Q, Ma J, Ge X M, Rao F, Ding K Y, Lv S L, Wu L C and Song Z T 2016 *Appl. Phys. Lett.* **108** 252102
[14] Zhu Y Q, Zhang Z H, Song S N, Xie H Q, Song Z T, Li X Y, Shen L L, Li L, Wu L C and Liu B 2015 *Mater. Res. Bull.* **64** 333
[15] Rao F, Song Z T, Ren K, Zhou X L, Cheng Y, Wu L C and Liu B 2011 *Nanotechnology* **22** 10
[16] Rao F, Ding K Y, Zhou Y X, Zheng Y H, Xia M J, Lv S L, Song Z T, Feng S L, Ronneberger I, Mazzarello R, Zhang W and Ma E 2017 *Science* **358** 1423
[17] Ren K, Xia M J, Rao F, Song Z T, Ding K Y, Ji X L, Wu L C, Liu B and Feng S L 2014 *Appl. Phys. Lett.* **104** 173102
[18] Ding K Y, Ren K, Rao F, Song Z T, Wu L C, Liu B and Feng S L 2014 *Mater. Lett.* **125** 143
[19] You H P , Hu Y F , Zhu X Q , Zou H , Song S N and Song Z T 2018 *Appl. Phys.* A **124** 168
[20] Hu Y F, He Z F, Zhai J W, Wu P Z, Lai T S, Song S N and Song Z T 2015 *Appl. Phys.* A **121** 1125
[21] He Z F, Wu P Z, Liu R R, Zhai J W, Lai T S, Song S N and Song Z T 2016 *CrystEngComm* **18** 1230
[22] Kumar S, Singh D, Shandhu S and Thangaraj R 2012 *Appl. Surf. Sci.* **258** 7406
[23] You H P, Hu Y F, Zhu X Q and Zou H 2017 *J. Mater. Sci.: Mater. Electron.* **28** 5562
[24] Xue Y, Song S N , Yan S, Guo T Q, Shen L L, Wu L C, Song Z T and Feng S L 2017 *J. Alloys Compd.* **727** 1288
[25] Hu Y F, Zhu X Q, Zou H, Lu Y, Xue J Z, Sui Y X, Wu W H, Yuan L, Song S N and Song Z T 2015 *J. Mater. Sci.: Mater. Electron.* **26** 7757